Structural Dynamics of DNA Depending on Methylation Patterns

Takeru Kameda,[1,2] Miho M. Suzuki,[3] Akinori Awazu,[4] and Yuichi Togashi[4,5,*]

[1] *Graduate School of Science, Hiroshima University, Higashi-Hiroshima, Hiroshima, Japan*
[2] *RIKEN Center for Biosystems Dynamics Research (BDR), Wako, Saitama, Japan*
[3] *Graduate School of Medicine, Nagoya University, Nagoya, Aichi, Japan*
[4] *Graduate School of Integrated Sciences for Life, Hiroshima University, Higashi-Hiroshima, Hiroshima, Japan*
[5] *RIKEN Center for Biosystems Dynamics Research (BDR), Higashi-Hiroshima, Hiroshima, Japan*

(Dated: June 30, 2020)

DNA methylation plays crucial roles in epigenetic regulation of eukaryotic gene expression. It is also suggested that methylation alters mechanical properties of DNA. However, most studies focused only on the roles of methylation at transcription start sites. Details of such mechanical changes, particularly in case of partial methylation, have not been systematically investigated. In this research, to elucidate effects of methylation on DNA mechanics, we performed fully atomic molecular dynamics simulation of double-stranded DNA with several patterns of methylation. Through the analysis of relative positioning of nucleotides (base-step variables), we observed characteristic changes in terms of local flexibility, which further affect the overall DNA geometry and stiffness. Our finding may serve as a basis for discussion about methylation-dependent DNA dynamics in physiological condition.

I. INTRODUCTION

DNA methylation is universal biochemical modification of DNA [1, 2]. A methyl group ($-CH_3$) binds to the cytosine base in a CpG dinucleotide, referred to as mCpG [1]. When a promoter region of a gene is methylated, expression of the gene is suppressed. mCpG is known to be recognized by some heterochromatin-related proteins [3]. Selective methylation can control which genes to be expressed, resulting in cell differentiation [4].

Methylated DNA (mCpG) is observed not only in promoter but over entire genome in mammals [5, 6], and hence biological roles beyond gene silencing have been proposed. For example, DNA methylation protects genome from activation of transposable elements [7, 8]. Although methylated DNA is included in genomes of higher organisms and thought to be important for many genomic functions, the abundance of mCpG varies and is correlated with the evolutionary pathway [4, 9, 10].

Besides, it has been proposed that DNA methylation also affects DNA mechanics. For example, DNA methylation reduces flexibility of DNA [11], inhibits or facilitates DNA strand separation [12], attracts homologous DNA segments [13], and also affects dynamics of nucleosomes [14]. It is comparable with sequence-dependent mechanics of DNA [15, 16], which affects basal processes of molecular recognition [17].

Recently, general effects of methylation on DNA dynamics have been studied by molecular dynamics (MD) simulations [18]. However, to fully elucidate the correlation between eukaryotic evolution, abundance of mCpG, and DNA dynamics, dependence on the pattern of methylation should be also systematically considered. In this research, we aimed to investigate the dependence in detail using all-atom MD simulations. Through the analysis of relative positioning of nucleotides, we found characteristic modes of changes in terms of local flexibility, which further affect the overall DNA dynamics.

II. MATERIALS AND METHODS

A. Simulation Procedure

We employed all-atom MD simulations for double stranded DNA dynamics in solution. DNA structures were constructed by X3DNA [19, 20] with a helical parameter set obtained by *in vitro* experiments and X-ray crystal structure analysis [15, 21, 22]. The atomic coordinates of double-stranded DNA were generated according to a given DNA sequence (see [19, 20] for details). In this study, for simplicity, we used repeats of CpG dinucleotides, and regular patterns of methylation were introduced as shown in Table I. These DNA models were soaked into a 60 Å × 60 Å × 200 Å water box, neutralized by K^+, and added 150 mM KCl. TIP3P water model was employed. VMD [23] was used to infer missing atom coordinates, solvate the model, and visualize the structure throughout the study.

All the simulations were carried out using NAMD (version 2.13 multi-core with CUDA) [24]. CHARMM36 force-field (July 2017 update) was used; 5MC2 nucleotide patch was applied to 5-methylated cytosine (mC) (Fig. 1 (a)). Periodic boundary condition with Particle-Mesh Ewald electrostatics was employed. Cutoff 12 Å (with switching from 10 Å) was used for non-bonded interactions. Temperature and pressure were set at 300 K and 1 atm, respectively; Langevin thermostat (damping coefficient: 5/ps) and Langevin-piston barostat were adopted. After energy minimization (10000 steps), the system was

* togashi@hiroshima-u.ac.jp

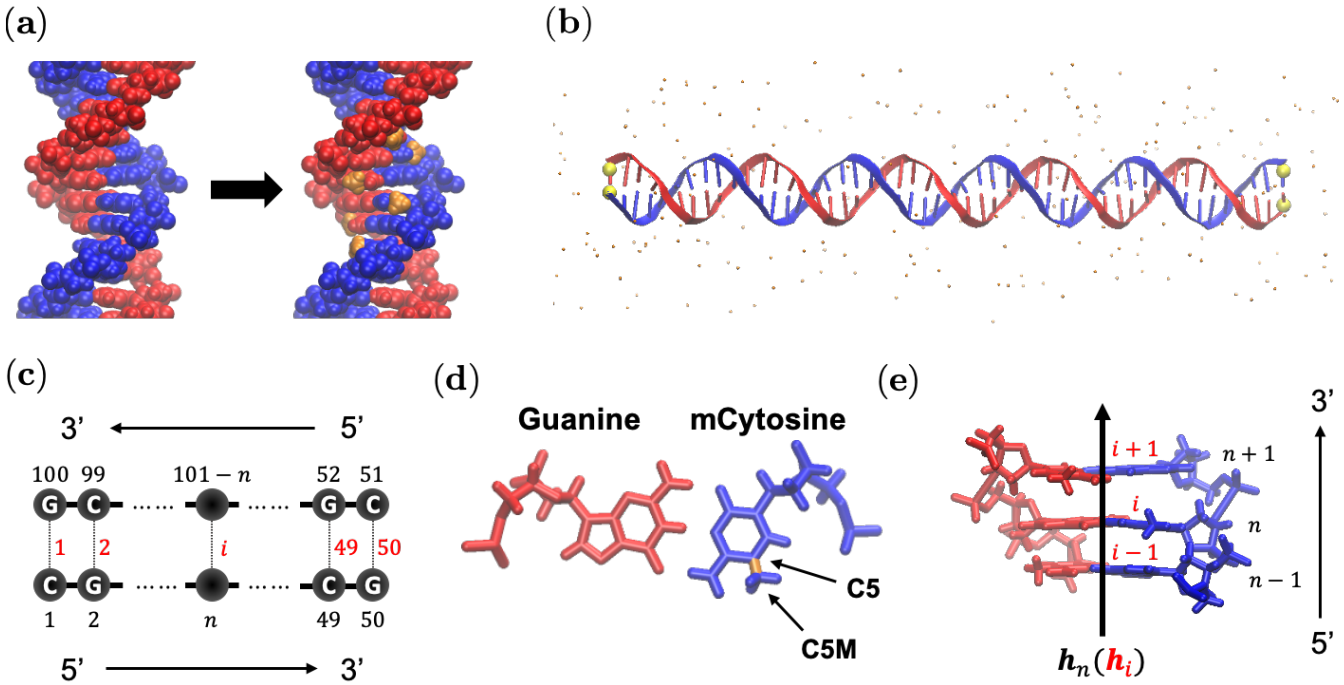

FIG. 1. Overview of the Model. (a) Structure of DNA with poly-CpG (left) and poly-mCpG (right). The methyl groups are shown in orange. (b) Solvated DNA model. Small particles represents ions. C1' atoms located at both ends (shown in yellow) are restrained in the simulation. (c) Nucleotide indices n (shown in black) and base-pair indices i (shown in red) of the double-stranded DNA. (d) Locations of C5 and C5M atoms in 5-methylated cytosine. (e) Schematic representation of helical axis $\boldsymbol{h_n}$ ($\boldsymbol{h_i}$).

equilibrated for 10 ns, and then simulated for 50 ns (time-step: 2 fs). The conformation was sampled over the last 50 ns at 10 ps intervals (i.e. 5000 snapshots), and each DNA model was simulated 10 times (i.e. 50000 snapshots in total). Through the equilibration and production run, harmonic restraints were applied to C1' atoms of nucleotides at both ends of the DNA segment (Fig. 1 (b); spring constant: 1.0 pN/Å). We confirmed that the restraints did not stretch the DNA excessively (Fig. 2 (c)).

B. Overall Geometry of DNA

Overall structural variation of the DNA model was characterized by the ratios of square root of the three principal components of the distribution of atomic positions, $\sqrt{\lambda_1}$, $\sqrt{\lambda_2}$, and $\sqrt{\lambda_3}$ ($\sqrt{\lambda_1} > \sqrt{\lambda_2} \geq \sqrt{\lambda_3}$ ¿ 0). Here, λ_1 to λ_3 were obtained as eigenvalues of the covariant matrix I:

$$I := \begin{pmatrix} \langle(\Delta x_k)^2\rangle_k & \langle\Delta x_k \Delta y_k\rangle_k & \langle\Delta x_k \Delta z_k\rangle_k \\ \langle\Delta y_k \Delta x_k\rangle_k & \langle(\Delta y_k)^2\rangle_k & \langle\Delta y_k \Delta z_k\rangle_k \\ \langle\Delta z_k \Delta x_k\rangle_k & \langle\Delta z_k \Delta y_k\rangle_k & \langle(\Delta z_k)^2\rangle_k \end{pmatrix} \quad (1)$$

where $(\Delta x_k, \Delta y_k, \Delta z_k) = (x_k - \langle x_m\rangle_m, y_k - \langle y_m\rangle_m, z_k - \langle z_m\rangle_m)$; (x_k, y_k, z_k) is the position of k-th atom, $(\langle x_m\rangle_m, \langle y_m\rangle_m, \langle z_m\rangle_m)$ is the center position of a given DNA molecule, and $\langle ...\rangle_m$ indicates the average for all ms. Note that $(\lambda_1, \lambda_2, \lambda_3)$ were defined for each snapshot τ, and thus 5000 data-points were obtained in each simulation trajectory (Section II A).

In this case, λ_1 and λ_2 correspond to the extension and distortion of double-stranded DNA, respectively.

C. Persistence Length of Double-Stranded DNA

Persistence length of polymers characterizes their stiffness statistically [25], and the case of double-stranded DNA has been studied well [26–28]. In this research, persistence length of DNA was defined as follows. First, A_d, inner-product of helical axes separated by d nm ($d \in [0.3, 10.0]$ at intervals 0.01) was defined as

$$A_d := \{\boldsymbol{h_i} \cdot \boldsymbol{h_j} \mid d - 0.005 \leq C_{ij} < d + 0.005\}$$
$$C_{ij} := \sum_{l=i}^{j-1} |\boldsymbol{c_{l+1}} - \boldsymbol{c_l}| \quad (2)$$
$$(11 \leq i < j \leq 40)$$

where $\boldsymbol{c_i}$ is the center of base pair i, and $\boldsymbol{h_i}$ is the helical axis of base-pair i (Fig. 1 (e)). These vectors were determined using X3DNA [19, 20]. To eliminate effects

TABLE I. Target Sequences. For each model, methylated CpG (mCpG) content ratio, and methylated cytosine (mC) sites are listed. All sequences were composed of only CpG dinucleotides. mC sites are indexed as shown in Fig. 1 (c).

Model	mCpG Content	mC Site (Nucleotide Indices)
SEQ 0.00	0% (0)	-
SEQ 0.25	25% (1/4)	1 9 17 25 33 41 49 51 59 67 75 83 91 99
SEQ 0.33	33% (1/3)	1 7 13 19 25 31 37 43 49 51 57 63 69 75 81 87 93 99
SEQ 0.50	50% (1/2)	1 5 9 13 17 21 25 29 33 37 41 45 49 51 55 59 63 67 71 75 79 83 87 91 95 99
SEQ 0.67	67% (2/3)	3 5 9 11 15 17 21 23 27 29 33 35 39 41 45 47 53 55 59 61 65 67 71 73 77 79 83 85 89 91 95 97
SEQ 0.75	75% (3/4)	3 5 7 11 13 15 19 21 23 27 29 31 35 37 39 43 45 47 53 55 57 61 63 65 69 71 73 77 79 81 85 87 89 93 95 97
SEQ 1.00	100% (1)	1 3 5 7 9 11 13 15 17 19 21 23 25 27 29 31 33 35 37 39 41 43 45 47 49 51 53 55 57 59 61 63 65 67 69 71 73 75 77 79 81 83 85 87 89 91 93 95 97 99

of the boundaries and restraints (Section II A), 10 base pairs from each end were eliminated (the base-pair indices (i, j) satisfy $11 \leq i < j \leq 40$). Then, the dataset $\{(d, \langle H \rangle_{H \in A_d})\}$ ($\langle ... \rangle_H$ indicates the average for all Hs, sampled over all the 5000 snapshots for each trial) was fitted by function $f(d) = \exp(-d/(2L))$, where L is the estimated persistence length.

D. Local Geometry and Flexibility

Profiles of base-step geometry were obtained by X3DNA [19, 20], from which the local flexibility was estimated. We focused on the displacement in terms of each mode from the (meta)stable conformation. Score $X_i^\bullet(\tau)$ for mode $\bullet$ of base pair i at τ-th frame, and its displacement $\hat{X}_i^\bullet(\tau)$ as $\hat{X}_i^\bullet(\tau) := X_i^\bullet(\tau) - X_i^\bullet(0)$ were calculated, where $X_i^\bullet(0)$ is the score $X_i^\bullet$ just after the energy minimization ($\tau = 0$) (see Section II A). Average and S.D. of $\hat{X}_i^\bullet(\tau)$ in each simulation trial, or over 10 trials for the same model, were evaluated.

E. Orientation of Methyl Group

Relative orientation of the methyl group was evaluated by the angle between the direction of methyl group and the plane formed by the base-pair. We define the angle θ_n as follows:

$$\begin{aligned} \theta_n &:= \theta_n^m - \theta_n^p \\ \theta_n^m &:= \cos^{-1}(\boldsymbol{h_n} \cdot \boldsymbol{d}_n^m) \\ \theta_n^p &:= \cos^{-1}(\boldsymbol{h_n} \cdot \boldsymbol{d}_n^p) \end{aligned} \tag{3}$$

where $\boldsymbol{h_n}$ is the vector of helical axis at the base-pair where nucleotide n belongs (Fig. 1 (e)), obtained by X3DNA [19, 20], $\boldsymbol{d}_n^m$ is the direction vector of methyl group (from C5 to C5M shown in Figure 1 (d)), and $\boldsymbol{d}_n^p$ is the direction vector from C1' atom to the C1' atom in the complementary base. The lengths of these 3 vectors equal to 1. If $\theta_n > 0$ ($\theta_n < 0$), the methyl group tilts toward the next (prior) base.

III. RESULTS

A. Profiles of Double-stranded DNA Stiffness

The overall geometry of DNA was represented by the extension ($\sqrt{\lambda_1}$) and distortion ($\sqrt{\lambda_2}$) of its atomic coordinates. Distribution of $\sqrt{\lambda_1}$ and $\sqrt{\lambda_2}$ for each model is shown in Figures 2 (a) and S1. Mostly, ($\sqrt{\lambda_1}$, $\sqrt{\lambda_2}$) is in the range of $47 \leq \sqrt{\lambda_1} \leq 49$ and $5 \leq \sqrt{\lambda_2} \leq 6$, corresponding to conformation similar to stretched DNA shape (e.g. Fig. 1 (b)).

On the other hand, the distribution out of this range was different for these models. The probability within this range is higher for SEQ 1.00 than for SEQ 0.00. $\sqrt{\lambda_2}$ of SEQ 1.00 tends to be smaller than that of SEQ 0.00. It implies that high mCpG content makes DNA shape stretched, or stiffer. The other models (Table I) showed intermediate stiffness between SEQ 0.00 and SEQ 1.00 (Figs. 2 (a) and S1). Variation of $\sqrt{\lambda_2}$ was suppressed as the mCpG content was increased. These results show that higher methylation content stiffens DNA in equilibrium condition.

Persistence length L (Section II C) for each model is shown in Fig. 2 (b), which increased with mCpG content, approximately linearly. Note that typical persistence length of DNA is about 50 nm ($\sim$ 150 base-pairs). Our estimated values were shorter, probably due to the restraints at the ends and the short (30 base-pairs) segment of measurement.

The difference of DNA stiffness could be observed also in the snapshots, as shown in Fig. 2 (c).

B. Local Base-Step Flexibility

The overall DNA geometry analyzed above is a result of sequential base-pair stacking [29, 30]. To investigate the effects of methylation in detail, we evaluated local profiles of flexibility at each base-step. Through the analysis using X3DNA (see Section II D), we obtained profiles of base-step geometry (Figure S2). We found that profiles of shift, tilt, and twist were most significantly changed,

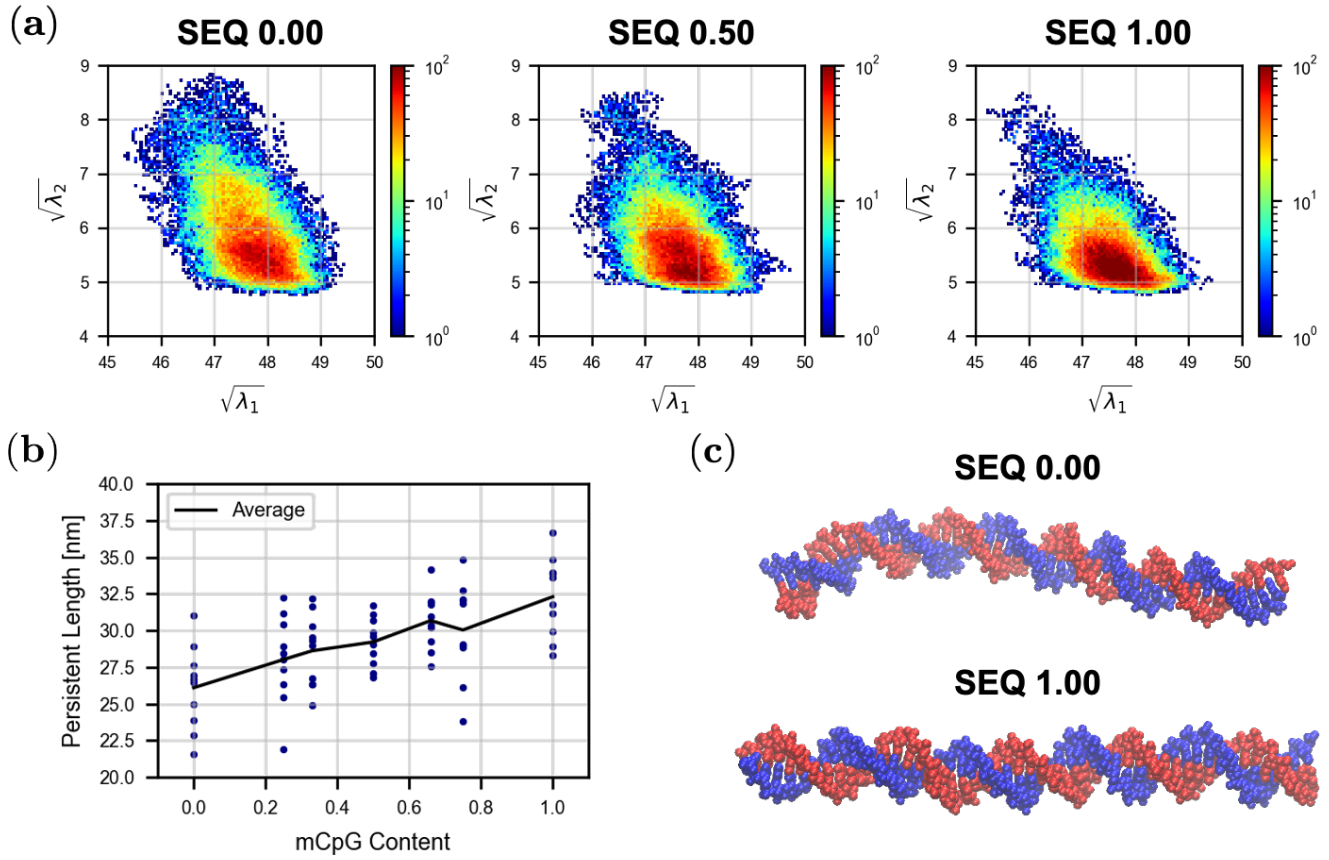

FIG. 2. Profiles of Overall Geometry and Persistence Length of DNA. (a) Overall geometry. Distribution of ($\sqrt{\lambda_1}$, $\sqrt{\lambda_2}$) summed over 10 trials is shown. (b) Persistence length L. Avarage in each trial and over 10 trials are shown. Horizontal axis corresponds to the mCpG content (Table I). (c) Snapshots of structure at 40 ns.

as shown in Fig. 3.

In the S.D. profiles of $\hat{X}_i^{shift}(\tau)$ and $\hat{X}_i^{tilt}(\tau)$, colored curves (i.e. 10 individual simulation trials) show alternating patterns, getting steeper as the mCpG content increases. More specifically, with higher mCpG content, S.D. of $\hat{X}_i^{shift}(\tau)$ and $\hat{X}_i^{tilt}(\tau)$ at base-steps G→C becomes smaller, while that at C→G is almost unchanged. As for the overall S.D. for the 10 trials, $\hat{X}_i^{tilt}(\tau)$ clearly shows alternating patterns similar to individual trials as the mCpG content increases, while $\hat{X}_i^{shift}(\tau)$ does not show such clear patterns. Taking into account the results of partially methylated cases (e.g. SEQ 0.50), methylated DNA makes tilt-mode stiffer at base-steps G→C, and restrict their deformation in some determined ranges.

Furthermore, mCpG suppresses tilt and shift dynamics only at the base-steps adjacent to the mCpG. In the profile of SEQ 0.33 in Fig. 3, S.D. of $\hat{X}_i^{tilt}(\tau)$ decreased at both neighbors of mCpG (Table I), while the S.D. is almost unchanged at G→C between non-methylated CpGs.

In contrast, for S.D. of $\hat{X}_i^{twist}(\tau)$, alternating patterns become less significant as mCpG content increases. In SEQ 0.00, S.D. of $\hat{X}_i^{twist}(\tau)$ at base-steps G→C is larger than at C→G, both in individual trials and overall S.D. On the other hand, in SEQ 1.00, the difference between G→C and C→G is smaller, and almost disappears in the overall S.D. profile. This result suggests that DNA methylation prevent twist dynamics irregularly. In general, DNA methylation makes twisting at base-steps G→C stiffer, however another considerable trend also exists. In SEQ 0.50, S.D. of $\hat{X}_i^{twist}(\tau)$ is actually higher at mCpG sites than at non-methylated CpG sites; this trend appears also in SEQ 0.33, although slightly. This result suggests that, in terms of twisting, methylation stiffens DNA in general, however C→G in the mCpG itself shows relatively large fluctuations.

C. Methyl Groups Distribution

Orientation of methyl group θ_n (Section II E) was evaluated, as shown in Fig. 4 (a). In any cases, θ_n distributes both positive and negative, and the average was about -0.2 [radian]. It suggests that methyl groups slightly tilt toward the 5'-end, however fluctuate much. We could not find any specific interactions (e.g. electrostatic interac-

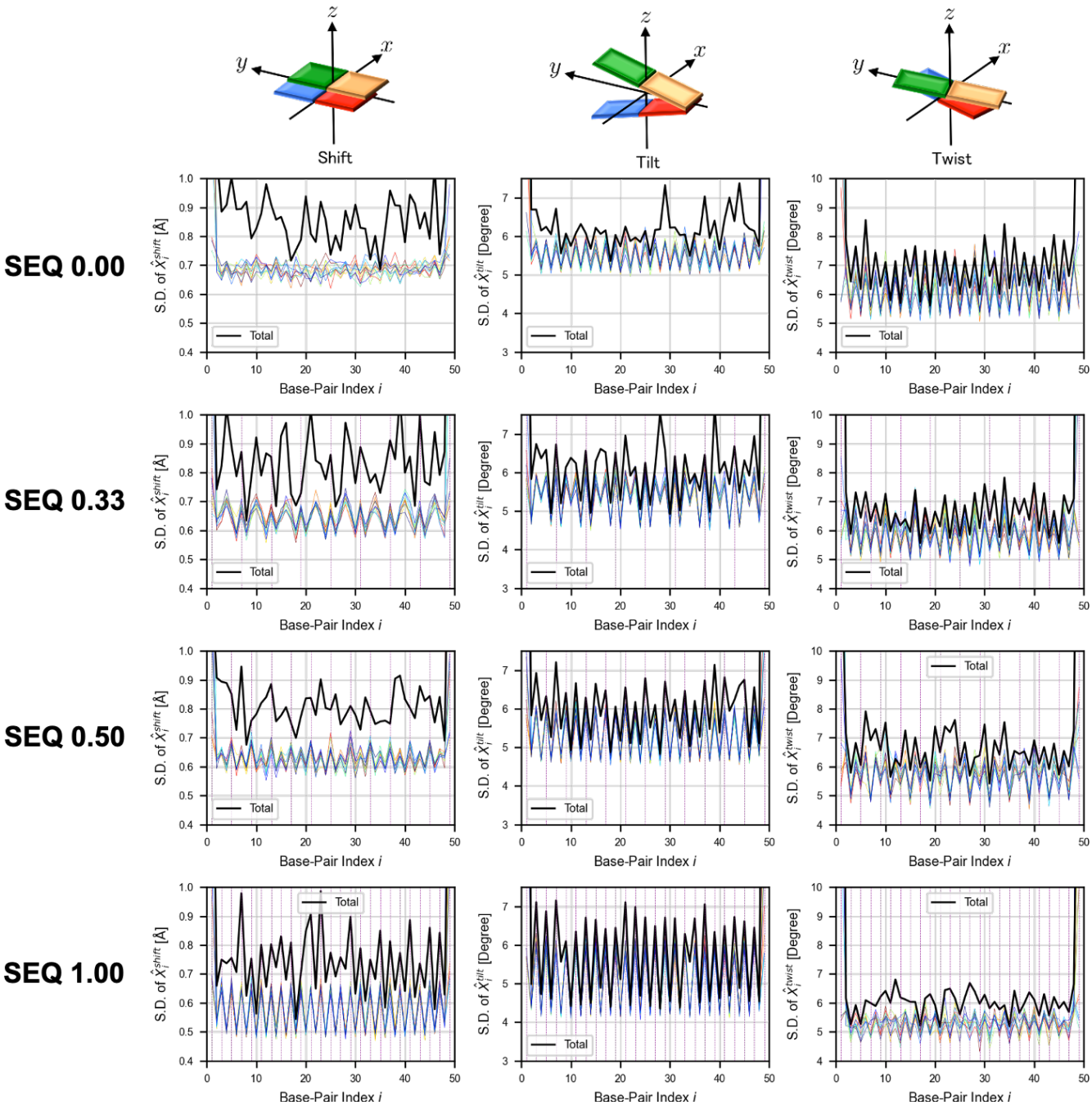

FIG. 3. Standard Deviation Profiles of $\hat{X}_i^{shift}(\tau)$, $\hat{X}_i^{tilt}(\tau)$ and $\hat{X}_i^{twist}(\tau)$. Colors show different simulation trials, and black line shows the overall S.D. for the 10 trials. In the horizontal axis, odd numbers and even numbers correspond to base steps of C→G and G→C, respectively. Purple lines show the mC sites.

tions) between the methyl group and other DNA parts, and hence it is suggested that weak van der Waals interactions and simple excluded volume effects play the role of changing local base-step flexibility.

IV. DISCUSSIONS

In this study, we investigated how different patterns of methylation affect DNA dynamics, both overall geometry and local flexibility at each base-step in terms of shift, tilt, or twist mode. Methylation generally stiffens DNA, which is consistent with preceding studies. Specifically,

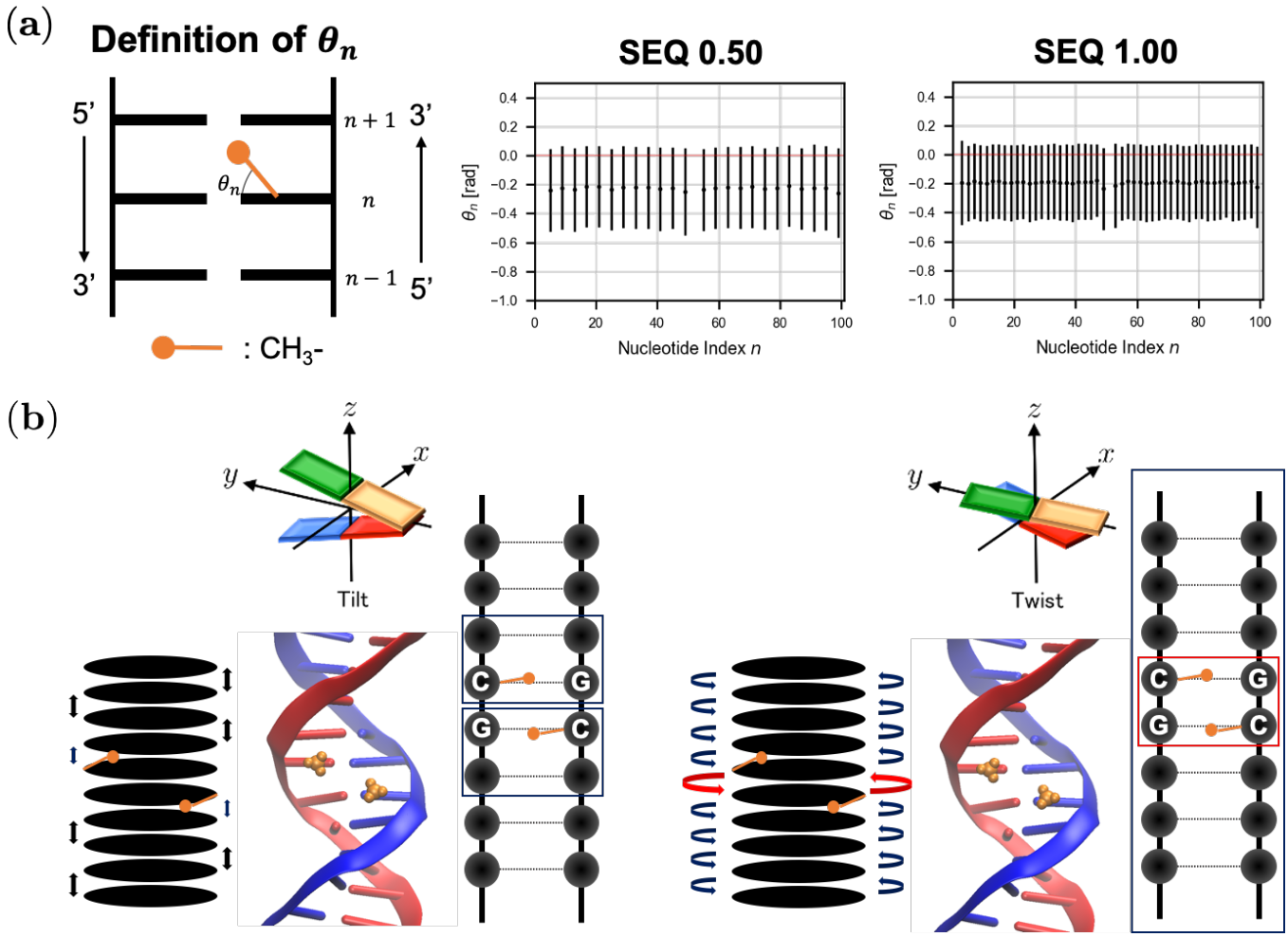

FIG. 4. Orientation of Methyl Groups and Suggested Effects. (a) Definition and observed distribution of θ_n. Average ± S.D. of θ_n for each methyl group are shown. (b) Suggested effects of DNA methylation on tilt and twist dynamics. Navy (or red) squares represent the ranges where site-specific DNA methylation (i.e. existence of mCpG) makes tilt or twist mode stiffer (or relatively flexible).

shifting and tilting dynamics of base-steps adjacent to mCpG was clearly restricted. Nevertheless, in terms of twisting, C→G base-steps in mCpG were certainly more flexible than other sites. This result might be originated from orientation of the methyl groups and their interactions with neighbors (Fig. 4 (b)). Twisting flexibility of C→G maintained at the mCpG itself might enhance accessibility of mCpG binding proteins [31, 32], although further investigations are required.

Previous findings suggest that DNA methylation stabilizes nucleosome positioning [33]. X-ray crystal structures of nucleosome have been obtained using special sequences of DNA, showing high affinity to core histones. In such nucleosome structures, DNA is not uniformly curved around histones but bent at several sites [34]. Our result also supports that site-specific DNA methylation may change local base-step flexibility, which may induce similar situation and enhance certain nucleosome positioning.

In our analysis, DNA methylation stiffens DNA globally (Fig. 2). It is also consistent with experiments [11]. Our finding suggests that effects of site-specific methylation on DNA dynamics should be evaluated not only just at the methylated site but also as global correlated dynamics (e.g. normal modes), as we previously proposed [35, 36]. In recent years, coarse-grained (reduced degree of freedom) physical models of DNA have been proposed, which also includes sequence-dependent mechanical properties (e.g. [35–38]). To reproduce dynamics of longer DNA in physiological conditions, methylation-dependent properties should be also incorporated into such models, which is also our future task.

DATA AVAILABILITY STATEMENT

AUTHOR CONTRIBUTIONS

TK, MS, AA, and YT conceived and designed the research and wrote the paper. TK, AA, and YT analyzed the data. TK and YT performed the simulations.

ACKNOWLEDGMENTS

The authors are grateful to I. Nikaido and S. Shinkai for fruitful discussions.

FUNDING

This work was supported by RIKEN Junior Research Associate Program, JSPS KAKENHI Grant Numbers JP16H01408, JP18H04720, and 18KK0388, and by JSPS and NRF under the Japan-Korea Basic Scientific Cooperation Program. A part of numerical calculations were carried out on the TSUBAME 3.0 supercomputer at Tokyo Institute of Technology, and RIKEN supercomputer HOKUSAI.

[1] D. N. Cooper, Human genetics **64**, 315 (1983).
[2] A. Bird, Cell **70**, 5 (1992).
[3] C. B. Klein and M. Costa, Mutation Research/Reviews in Mutation Research **386**, 163 (1997).
[4] Z. D. Smith and A. Meissner, Nature Reviews Genetics **14**, 204 (2013).
[5] M. J. Ziller, H. Gu, F. Müller, J. Donaghey, L. T.-Y. Tsai, O. Kohlbacher, P. L. De Jager, E. D. Rosen, D. A. Bennett, B. E. Bernstein, *et al.*, Nature **500**, 477 (2013).
[6] M. M. Suzuki and A. Bird, Nature Reviews Genetics **9**, 465 (2008).
[7] J. A. Yoder, C. P. Walsh, and T. H. Bestor, Trends in genetics **13**, 335 (1997).
[8] J. Barau, A. Teissandier, N. Zamudio, S. Roy, V. Nalesso, Y. Hérault, F. Guillou, and D. Bourc'his, Science **354**, 909 (2016).
[9] A. Zemach, I. E. McDaniel, P. Silva, and D. Zilberman, Science **328**, 916 (2010).
[10] V. Colot and J.-L. Rossignol, Bioessays **21**, 402 (1999).
[11] T. T. Ngo, J. Yoo, Q. Dai, Q. Zhang, C. He, A. Aksimentiev, and T. Ha, Nature communications **7**, 10813 (2016).
[12] P. M. Severin, X. Zou, H. E. Gaub, and K. Schulten, Nucleic acids research **39**, 8740 (2011).
[13] J. Yoo, H. Kim, A. Aksimentiev, and T. Ha, Nature communications **7**, 11045 (2016).
[14] I. Jimenez-Useche, J. Ke, Y. Tian, D. Shim, S. C. Howell, X. Qiu, and C. Yuan, Scientific reports **3**, 2121 (2013).
[15] W. K. Olson, A. A. Gorin, X.-J. Lu, L. M. Hock, and V. B. Zhurkin, Proceedings of the National Academy of Sciences **95**, 11163 (1998).
[16] M. Rief, H. Clausen-Schaumann, and H. E. Gaub, Nature structural biology **6**, 346 (1999).
[17] R. Rohs, S. M. West, A. Sosinsky, P. Liu, R. S. Mann, and B. Honig, Nature **461**, 1248 (2009).
[18] A. T. P. Carvalho, L. Gouveia, C. R. Kanna, S. K. T. S. Wärmländer, J. A. Platts, and S. C. L. Kamerlin, Epigenetics **9**, 1604 (2014).
[19] X.-J. Lu and W. K. Olson, Nucleic acids research **31**, 5108 (2003).
[20] X.-J. Lu and W. K. Olson, Nature protocols **3**, 1213 (2008).
[21] W. K. Olson, A. V. Colasanti, Y. Li, W. Ge, G. Zheng, and V. B. Zhurkin, in *Computational Studies of RNA and DNA* (Springer, 2006) pp. 235–257.
[22] A. V. Morozov, K. Fortney, D. A. Gaykalova, V. M. Studitsky, J. Widom, and E. D. Siggia, Nucleic acids research **37**, 4707 (2009).
[23] W. Humphrey, A. Dalke, and K. Schulten, J. Mol. Graph. **14**, 33 (1996).
[24] J. C. Phillips, R. Braun, W. Wang, J. Gumbart, E. Tajkhorshid, E. Villa, C. Chipot, R. D. Skeel, L. Kale, and K. Schulten, J. Comput. Chem. **26**, 1781 (2005).
[25] P. J. Flory and M. Volkenstein, Biopolymers: Original Research on Biomolecules **8**, 699 (1969).
[26] J. Bednar, P. Furrer, V. Katritch, A. Stasiak, J. Dubochet, and A. Stasiak, Journal of molecular biology **254**, 579 (1995).
[27] P. Gross, N. Laurens, L. B. Oddershede, U. Bockelmann, E. J. Peterman, and G. J. Wuite, Nature Physics **7**, 731 (2011).
[28] G. S. Manning, Biophysical journal **91**, 3607 (2006).
[29] C. Calladine, Journal of molecular biology **161**, 343 (1982).
[30] C. A. Hunter, Journal of molecular biology **230**, 1025 (1993).
[31] I. Ohki, N. Shimotake, N. Fujita, J.-G. Jee, T. Ikegami, M. Nakao, and M. Shirakawa, Cell **105**, 487 (2001).
[32] X. Zou, W. Ma, I. A. Solov'Yov, C. Chipot, and K. Schulten, Nucleic acids research **40**, 2747 (2012).
[33] R. K. Chodavarapu, S. Feng, Y. V. Bernatavichute, P.-Y. Chen, H. Stroud, Y. Yu, J. A. Hetzel, F. Kuo, J. Kim, S. J. Cokus, *et al.*, Nature **466**, 388 (2010).
[34] C. A. Davey, D. F. Sargent, K. Luger, A. W. Maeder, and T. J. Richmond, Journal of molecular biology **319**, 1097 (2002).
[35] S. Isami, N. Sakamoto, H. Nishimori, and A. Awazu, PLoS one **10**, e0143760 (2015).
[36] T. Kameda, S. Isami, Y. Togashi, H. Nishimori, N. Sakamoto, and A. Awazu, Frontiers in physiology **8**, 103 (2017).
[37] P. Šulc, F. Romano, T. E. Ouldridge, L. Rovigatti, J. P. Doye, and A. A. Louis, The Journal of chemical physics **137**, 135101 (2012).
[38] G. S. Freeman, D. M. Hinckley, J. P. Lequieu, J. K. Whitmer, and J. J. de Pablo, The Journal of chemical physics **141**, 165103 (2014).